

Direct detections of Majorana dark matter in vector portal

Wei Chao^{1*}

¹*Center for Advanced Quantum Studies, Department of Physics,
Beijing Normal University, Beijing, 100875, China*

Abstract

In this paper we investigate the direct detections of Majorana dark matter (MDM) in vector portal. Taking into account that the tree-level scattering cross sections in these models are either dark matter velocity suppressed or spin-dependent, we calculate radiative corrections to the spin-independent cross section in effective field theory approach. Wilson coefficients of effective MDM-quark interactions are calculated at the one-loop level, and the Wilson coefficient of the effective MDM-gluon interaction is derived at the two-loop level. Numerical results show that current constraints can rule out a narrow mass range of MDM when tree-level contributions are considered, and the spin-independent cross section from radiative corrections is reachable by the current direct detection technique for light MDM.

arXiv:1904.09785v1 [hep-ph] 22 Apr 2019

* chaowei@bnu.edu.cn

I. INTRODUCTION

Various observations have confirmed the existence of dark matter in our universe, whose relic density, derived by measuring the cosmic microwave background, large scale structure and galaxy formation, is about 0.1198 ± 0.0033 [1]. The standard model (SM) of particle physics contains no cold dark matter candidate, and the nature of dark matter remains elusive. There are many dark matter candidates with masses ranging from 10^{-20} eV to 10^{55} GeV, of which the weakly interacting massive particle (WIMP) [2–7] is well-motivated as it can naturally explain the observed relic density via the thermal freeze-out with its mass at the electroweak scale and with weak couplings to the SM particles.

There are three (direct or indirect) ways of detecting WIMPs in laboratories: looking for the scattering between WIMPs and nucleon in underground laboratories by measuring the nuclear recoil energy in the kilo-electronvolt scale, detecting the flux of cosmic rays injected by the WIMP annihilations or decays with the help of satellites or telescopes, and producing WIMPs at the Large Hadron Collider (LHC) where the signal of WIMP is missing transverse momentum or missing energy. Of these three efforts, the first detection method is most straightforward since the astrophysical sources of cosmic rays have not been clearly determined in indirect detection experiments, and LHC is actually a mediator machine in dark matter detections.

Benefiting from technological advances, direct detection experiments such as LUX [8], PandaX-II [9] and XENON1T [10] have made tremendous strides in increasing precision and detecting efficiency. In an ideal status, one can detect arbitrarily small direct detection cross section by continuously increasing the exposure, however it is well-known that direct detection experiments will soon reach an irreducible background from coherent elastic neutrino-nuclei scattering, the so-called “neutrino floor” [11]. The current direct detection techniques will not be able to distinguish the signal of dark matter from that of neutrinos if the signal lies below the neutrino floor. That is to say the neutrino floor is the border of new and “old” direct detection techniques. As a result, the precision calculation of the direct detection cross sections will be important, if one wants to examine as many dark matter models as possible with the help of current direct detection techniques.

In this paper, we study the direct detections (DD) of a vector portal Majorana dark matter (MDM) [12]. The vector mediator model is one of the simplest models, whose

phenomenology has been widely studied in Refs. [13–23]. In this model χ is a Majorana dark matter, V_μ is a vector mediator, whose mass may arise from the spontaneous breaking of certain $U(1)$ gauge symmetry, and V_μ may couple to the SM via a vector current or axial-vector current. In some models the vector portal is associated with the Higgs portal since the scalar that causes the spontaneous breaking of the new $U(1)$ gauge symmetry may mix with the SM Higgs. Here we assume the mixing is negligibly small, thus the scattering of χ off the nuclei is only mediated by the V_μ . The direct detection cross section σ is either spin-independent but suppressed by the dark matter velocity or spin-dependent [24, 25]. As a result, the spin-independent cross section σ_{SI} , generated at the loop level [26–38], turns out to be important as it may be still possible to examine these models with the current DD technique if σ_{SI} lies above the neutrino floor. We calculate effective operators for the evaluation of MDM-nucleon spin independent scattering cross section following [39, 40]. The WIMP-gluon effective operator [41, 42] arising at the two-loop level is also derived. Numerical simulations show that the σ_{SI} from radiative corrections is reachable by the current DD technique for light MDM.

The remaining of the paper is organized as follows: In section II we give a brief introduction to the vector portal MDM model. Section III is focused on the calculation of Wilson coefficients of effective operators. Numerical results are presented in section IV and the last part is concluding remarks. Expressions of loop functions are listed in the appendix A. Nuclear form factors are given in the appendix B.

II. THE MODEL

In this section, we review the vector portal dark matter model. The simplified model contains a Majorana fermion χ and a new vector boson V_μ in addition to the SM particles. The Lagrangian for χ can be written as

$$\mathcal{L}_\chi = \frac{1}{2}\bar{\chi}i\not{\partial}\chi + \frac{1}{2}g_V\bar{\chi}\gamma^\mu\gamma^5V_\mu\chi - \frac{1}{2}m_\chi\bar{\chi}\chi \quad (1)$$

where m_χ is the dark matter mass, g_V is the new gauge coupling. The ultraviolet completed model contains a $U(1)$ gauge symmetry and a complex scalar $\Phi(\equiv \frac{1}{\sqrt{2}}(\phi + iG + v_\Phi))$ which is charged under the new $U(1)$ and whose vacuum expectation value (VEV) v_Φ leads to the spontaneous breaking of the new gauge symmetry and the origin of masses of χ and V .

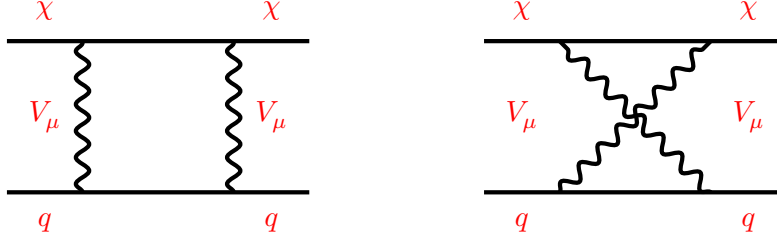


FIG. 1: Box diagrams for the effective quark-WIMP interactions

In this case there will be a new Yukawa interaction, $\frac{1}{2}y_\chi\overline{\chi}_A^C\Phi\chi_A + \text{h.c.}$, where the subindex A represents the chirality, and Eq.(1) needs to be extended with the $\frac{1}{2}\overline{\chi}\phi\chi$ term. In the case where ϕ mixes with the SM Higgs, there will be Higgs portal interactions. Notice that the mixing is caused by the quartic term: $\lambda_{H\Phi}\Phi^\dagger\Phi H^\dagger H$. $\lambda_{H\Phi}$ should be small when taking into account constraints from precision observables as well as Higgs measurements at the LHC. Here we assume the mixing is negligible.

For interactions of new gauge boson with the SM particles, V_μ may couple to vector bilinears or axial-vector bilinears, or both, depending on the $U(1)$ charge settings of the SM fermions. For example, new gauge interactions are $g_V\bar{f}\gamma^\mu f$ in $U(1)_{B-L}$ [43], $U(1)_{B+L}$ [44] and $U(1)_{B_i-L_j}$ models. While in the model where two chiral components carry opposite $U(1)$ charges, new gauge interactions will be $g_V\bar{f}\gamma^\mu\gamma^5 f$. If only one certain chirality component carries non-zero charge, new gauge interactions will be $g_V\bar{f}\gamma^\mu P_A V_\mu f$ [45], where $P_A = P_L$ or P_R . In this paper we carry out model independent study and investigate the DD cross section of vector current and axial-vector current scenarios separately. Interactions of V_μ with quarks are then

$$\mathcal{L}_I^q \in \zeta g_V \bar{q} \gamma^\mu q V_\mu, \text{ (scenario A)} \quad (2)$$

$$\mathcal{L}_{II}^q \in \zeta g_V \bar{q} \gamma^\mu \gamma^5 q V_\mu, \text{ (scenario B)} \quad (3)$$

where ζ is the $U(1)$ hyper-charge of the quark q . Free parameters in these models are thus m_χ , m_V , g_X and ζ .

III. EFFECTIVE OPERATORS

In this section we calculate effective operators relevant for the spin-independent scattering cross section of χ with a nucleon. Following Refs. [39, 40], we write down the effective χ -

quark interactions in terms of the higher-dimensional operators:

$$\mathcal{L}_{\text{eff}} = \kappa_0 \bar{\chi} \gamma^\mu \gamma^5 \chi \bar{q} \Gamma q + \sum_{p=q,g} \frac{1}{2} \kappa_{1p} \bar{\chi} \chi \mathcal{O}_s^p + \frac{1}{2} \kappa_{2q} \bar{\chi} i \partial^\mu \gamma^\nu \chi \mathcal{O}_{\mu\nu}^q + \frac{1}{2} \kappa_{3q} \bar{\chi} i \partial^\mu i \partial^\nu \chi \mathcal{O}_{\mu\nu}^q, \quad (4)$$

where $\Gamma = \gamma^\mu$ for scenario A, $\Gamma = \gamma^\mu \gamma^5$ for scenario B, κ_{ip} are wilson coefficients, $\mathcal{O}_s^q = m \bar{q} q$, $\mathcal{O}_s^g = -\frac{9}{8} \alpha_s G^{A\mu\nu} G_{\mu\nu}^A$ and $\mathcal{O}_{\mu\nu}^q$ are twist-2 operators, defined by

$$\mathcal{O}_{\mu\nu}^q = \frac{1}{2} \bar{q} \left(\partial_\mu \gamma_\nu + \partial_\nu \gamma_\mu - \frac{1}{2} g_{\mu\nu} \not{\partial} \right) q. \quad (5)$$

These effective operators are defined at the mass scale of V_μ , which is assumed to be heavier than all the SM particles. In the following, we calculate Wilson coefficients at the leading order.

The leading contribution to the Wilson coefficient κ_0 arises from the tree level diagram by exchanging the vector boson V_μ ,

$$\kappa_0 = \frac{\zeta g_V^2}{2m_V^2}, \quad (6)$$

where m_V is the mass of V_μ .

$\kappa_{1,2,3}^q$ arise from the box diagrams shown in the Fig. 1. We calculate the diagrams in the zero-momentum transfer limit, and expand the amplitude in term of the quark momentum, which is non-relativistic, then we decompose results into effective operators following [37].

For the scenario A, the relevant Wilson coefficients are

$$\begin{aligned} \kappa_{A1q} = & -\frac{m_\chi}{2} \alpha_V^2 \{ 3X_2(m_\chi^2, m_V^2, 0, m_\chi^2) + Y_2(m_\chi^2, m_V^2, 0, m_\chi^2) + 12Z_{001}(m_\chi^2, m_V^2, m_\chi^2) \\ & + 6Z_{00}(m_\chi^2, m_V^2, m_\chi^2) + m_\chi^2 [3Z_{11}(m_\chi^2, m_V^2, m_\chi^2) + 2Z_{111}(m_\chi^2, m_V^2, m_\chi^2)] \} \end{aligned} \quad (7)$$

$$\begin{aligned} \kappa_{A2q} = & -2\alpha_V^2 \{ 2Z_{00}(m_\chi^2, m_V^2, m_\chi^2) + 8Z_{001}(m_\chi^2, m_V^2, m_\chi^2) + m_\chi^2 [Z_{11}(m_\chi^2, m_V^2, m_\chi^2) \\ & + Z_{111}(m_\chi^2, m_V^2, m_\chi^2)] - X_2(m_\chi^2, m_V^2, 0, m_\chi^2) - Y_2(m_\chi^2, m_V^2, 0, m_\chi^2) \} \end{aligned} \quad (8)$$

$$\kappa_{A3q} = -2\alpha_V^2 [2Z_{11}(m_\chi^2, m_V^2, m_\chi^2) + Z_{111}(m_\chi^2, m_V^2, m_\chi^2)] \quad (9)$$

where $\alpha_V = g_V^2/4\pi$. The definitions of the loop functions and their explicit expressions are given in the appendix A. Loop functions are evaluated with the help of the Package-X [48, 49].

For scenario B the Wilson coefficients are

$$\begin{aligned} \kappa_{B1q} = & +\frac{m_\chi}{2} \alpha_V^2 \{ 9X_2(m_\chi^2, m_V^2, 0, m_\chi^2) + 3Y_2(m_\chi^2, m_V^2, 0, m_\chi^2) - 6Z_{00}(m_\chi^2, m_V^2, m_\chi^2) \\ & + 13Z_{001}(m_\chi^2, m_V^2, m_\chi^2) - m_\chi^2 [3Z_{11}(m_\chi^2, m_V^2, m_\chi^2) - 2Z_{111}(m_\chi^2, m_V^2, m_\chi^2)] \} , \end{aligned} \quad (10)$$

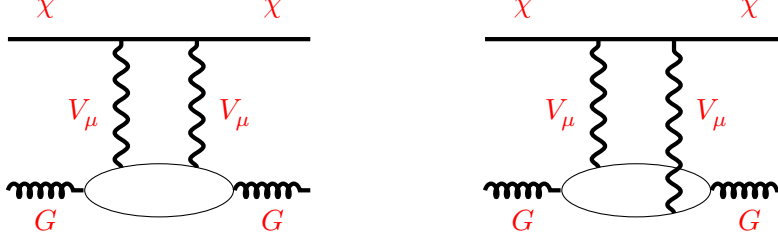


FIG. 2: Two-loop Feynman diagrams for the effective gluon-WIMP interactions.

$$\kappa_{B2q} = -2\alpha_V^2 \{ 2Z_{00}(m_\chi^2, m_V^2, m_\chi^2) - 8Z_{001}(m_\chi^2, m_V^2, m_\chi^2) + m_\chi^2 [Z_{11}(m_\chi^2, m_V^2, m_\chi^2) - Z_{111}(m_\chi^2, m_V^2, m_\chi^2)] - X_2(m_\chi^2, m_V^2, 0, m_\chi^2) - Y_2(m_\chi^2, m_V^2, 0, m_\chi^2) \} , \quad (11)$$

$$\kappa_{B3q} = -2\alpha_V^2 [2Z_{11}(m_\chi^2, m_V^2, m_\chi^2) - Z_{111}(m_\chi^2, m_V^2, m_\chi^2)] . \quad (12)$$

The effective MDM-gluon interactions arise at the two-loop level. Relevant Feynman diagrams are given in the Fig. 2. In this paper we only take into account the effect of twist-0 operator while neglecting that of higher twist operators. One loop correction to the two-point function of gauge boson in the gluon background field has been calculated in Ref. [46] by taking the Fock-Schwinger gauge [50, 51] for the gluon field, which, mapped into our cases, can be written as

$$i\Pi_{VV}^{(f)\alpha\beta} = -\frac{1}{3} \frac{i\zeta^2 g_s^2}{16\pi} G_{\mu\nu}^a G^{a\mu\nu} \left(\frac{g_V^2}{q^2} g^{\alpha\beta} - \frac{g_V^2}{q^4} q^\alpha q^\beta \right) \quad (13)$$

where g_s is the coupling of the strong interaction, f indicates the flavor running in the fermion loop, q is the momentum of gauge boson. Notice that Eq. (13) is universal for both the scenario A and scenario B.

With the help of Eq. (13), one can write down the Wilson coefficient of the effective χ -gluon operator as

$$\kappa_{Ag(Bg)} = \frac{\alpha_V^2}{54} \zeta^2 n_f m_\chi \left(6X_2(m_\chi^2, m_V^2, 0, m_\chi^2) + 2Y_2(m_\chi^2, m_V^2, 0, m_\chi^2) + 6Z_{001}(m_\chi^2, m_V^2, m_\chi^2) - 6Z_{00}(m_\chi^2, m_V^2, m_\chi^2) + m_\chi^2 Z_{11}(m_\chi^2, m_V^2, m_\chi^2) \right) \quad (14)$$

where n_f is the number of quarks that carry nonzero U(1) charge.

Wilson coefficients given above are matched to the simplified model at $\mu \approx m_V$. The energy scale for the DM direct detections is about the nuclear energy scale. It has been shown in Ref. [28] that effects from the running of renormalization group equations might be sizable in certain vector-portal scenario. We use the public code RUNDM [28] to evolve the running of κ_0 and evaluate running effects of other Wilson coefficients following Refs. [42, 52–55].

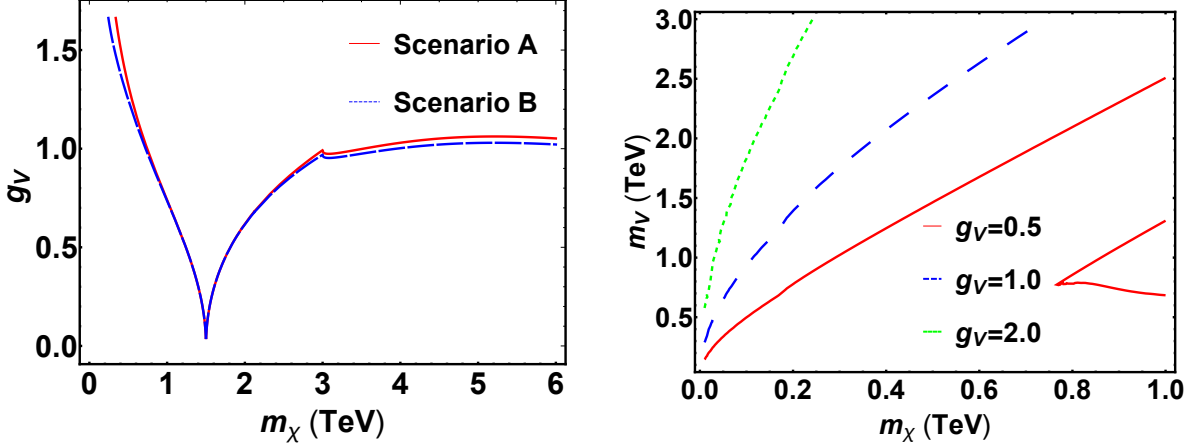


FIG. 3: Left panel: New gauge coupling as the function of the dark matter mass by setting $m_V = 3$ TeV and $\zeta = 1$, constrained by the observed relic density. The solid and dashed lines correspond to the scenario I and scenario II respectively. Right panel: Contours of g_V in the $m_\chi - m_V$ plane by setting $\zeta = 1$.

IV. RESULTS

In this section we present results for the MDM-nucleon scattering cross section. We start by determining the g_V using the observed relic density. As was mentioned in the previous section, there are four parameters in the vector portal, which are all relevant for both the relic abundance and the direct detection cross section. The thermal relic abundance is determined by the following processes: $\bar{\chi}\chi \rightarrow \bar{f}f$ and $\bar{\chi}\chi \rightarrow V_\mu V^\mu$, where f indicates the SM fermion. The first channel depends on the parameter ζ , while the second channel does not. For $m_\chi < m_V$, the channel $\bar{\chi}\chi \rightarrow V_\mu V^\mu$ is kinematically forbidden, and thus the combination ζg_V^2 can be determined in this mass range.

We show in the Fig. 3, the new gauge coupling g_V as the function of the dark matter mass m_χ determined by the observed relic abundance $\Omega h^2 = 0.1198$, by setting $m_V = 3$ TeV and $\zeta = 1$. The solid line and dashed line correspond to cases of scenario A and scenario B, respectively. The first dip of the plot appears at $m_\chi \sim m_V/2$, where the annihilation $\bar{\chi}\chi \rightarrow \bar{f}f$ is resonantly enhanced. The second dip of the plot at $m_\chi \sim m_V$ is due to the opening of the channel $\bar{\chi}\chi \rightarrow V_\mu V^\mu$. Notice that g_V becomes almost scenario independent as $m_\chi \sim m_V$. We show in the right panel of the Fig. 3 contours of g_V in the $m_\chi - m_V$ plane by setting $\zeta = 1$. Notice that $\mathcal{O}(g_V) \sim 1$ for $m_V \sim m_\chi \sim \mathcal{O}(1)$ TeV.

We show in the Fig. 4 Wilson coefficients as the function of the dark matter mass m_χ by

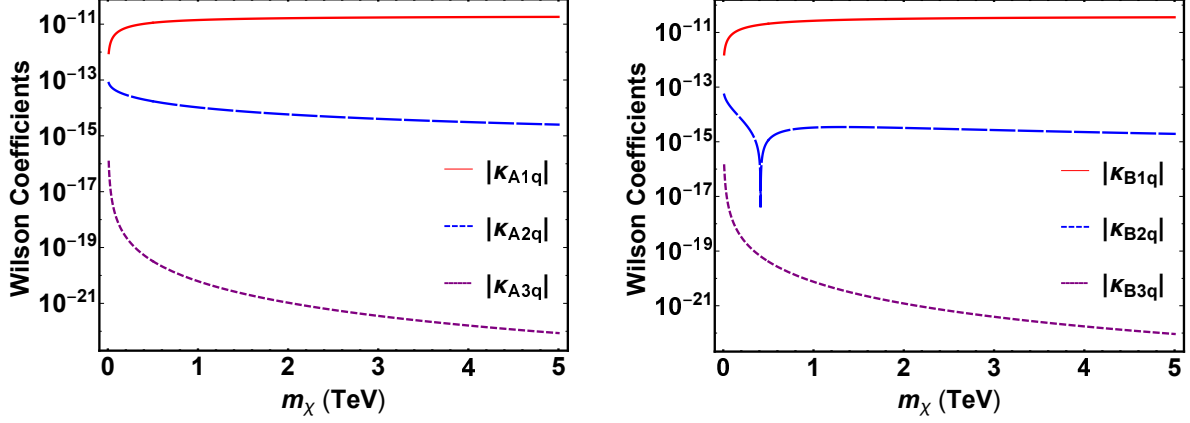


FIG. 4: Wilson coefficients as the function of the dark matter mass by setting $\zeta = g_V = 1$ and $m_V = 1$ TeV for scenario A (left-panel) and scenario B (right-panel).

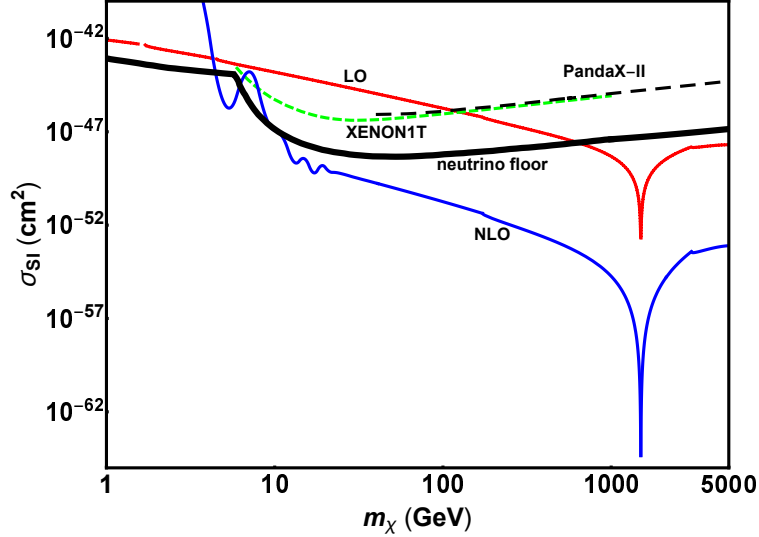


FIG. 5: Direct detection cross section as the function of the dark matter mass by setting $\zeta = 1$ and $m_V = 3$ TeV for scenario A. The red solid and blue dashed lines correspond to the LO and NLO contributions respectively. The black dashed and green dashed lines are separately constraints of Pandax-II and XENON1T.

setting $g_V = \zeta = 1$ and $m_V = 1$ TeV. The plot in the left-panel and right-panel correspond to cases of scenario A and B respectively. As can be seen, the Wilson coefficient of the scalar type interaction is largest and is comparable to that in pseudo-scalar portal model [37]. Wilson coefficients in scenario B is similar to these in scenario A except κ_{B2q} at $m_\chi \sim m_V$, which is due to the cancellation of various contributions. The Wilson coefficient κ_g is of the order $\mathcal{O}(10^{-11})$ by setting $g_V = \zeta = 1$.

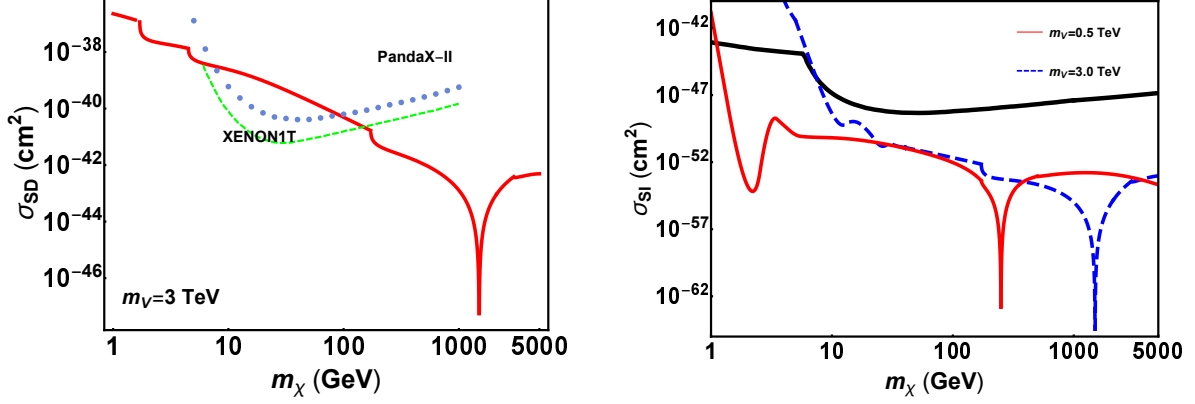


FIG. 6: Left-panel: Spin-dependent χ -neutron scattering cross section as the function of the dark matter mass by setting $\zeta = 1$ and $m_V = 3$ TeV for scenario B. The red and blue dotted lines are constraints of XENON1T and PandaX-II, respectively. Right-panel: spin-independent χ -neutron scattering cross section as the function of m_χ by setting $\zeta = 1$ and $m_V = 3$ TeV for scenario B.

Now we calculate the MDM-nucleon scattering cross section. For scenario A, there is velocity suppressed spin-independent scattering cross section at the leading order,

$$\sigma_{\text{SI}}^{\text{LO}} \approx \frac{36\pi\zeta^2\alpha_V^2\mu^2v^2}{m_V^4}, \quad (15)$$

where μ is the reduced mass of χ and nucleon system, v is the velocity of the dark matter. Effective interactions given in the Eq. (4) contribute to the scattering cross section at the next-to-leading order,

$$\sigma_{\text{SI}}^{\text{NLO}} = \frac{\mu^2 m_N^2}{\pi} \left[\sum_q \kappa_{A1q} f_{Tq}^N + \kappa_g f_{Tg}^N + \frac{3}{4} \sum_q (m_\chi \kappa_{A2q} + m_\chi^2 \kappa_{A3q}) (q^N(2) + \bar{q}^N(2)) \right]^2 \quad (16)$$

where N stands for (p, n) with m_N its mass, f_{Tq}^N is the quark matrix element defined by $\langle N | m_q \bar{q}q | N \rangle = m_N f_{Tq}^N$, f_{Tg}^N is the gluon matrix element defined by $-\frac{9\alpha_s}{8\pi} \langle N | G_{\mu\nu}^a G^{a\mu\nu} | N \rangle = m_N f_{Tg}^N$, $q^N(2)$ and $\bar{q}^N(2)$ are second moments for quark distribution functions of N . Numerical values of f_{Tq}^N , f_{Tg}^N as well as $q^N(2)$ and $\bar{q}^N(2)$ are listed in the appendix B. Notice that there is no interference between the leading order and the next to leading order contributions. As a result, the total cross section for scenario A can be written as $\sigma_{\text{SI}}^{\text{tot}} = \sigma_{\text{SI}}^{\text{LO}} + \sigma_{\text{SI}}^{\text{NLO}}$.

For scenario B, the χ -nucleon scattering cross section is spin-dependent at the leading order,

$$\sigma_{\text{SD}}^{\text{LO}} = 64\pi\zeta^2\alpha_V^2\frac{\mu^2}{m_V^4} \left(\sum_q \Delta_q^N \right)^2 J_N(J_N + 1) \quad (17)$$

where Δ_q^N is the spin fraction of quark q , defined by $2\Delta_q^N s^\mu = \langle N | \bar{q} \gamma^\mu \gamma^5 | N \rangle$ with s^μ the nucleon spin four-vector, J_N is the angular momentum of the nucleon. Δ_q^N are measured in DIS and one has $\Delta_u^p = 0.77$, $\Delta_d^p = -0.47$ and $\Delta_s^p = -0.15$ [47]. The χ -nucleon scattering cross section at the next-to-leading order can be spin independent, whose expression is the same as eq. (16), up to replacements, $\kappa_{Aiq} \rightarrow \kappa_{Biq}$ ($i = 1, 2, 3$).

As an illustration, we show in the Fig. 5 the direct detection cross section as the function of the dark matter mass m_χ for scenario A, by setting $m_V = 3$ TeV and $\zeta = 1$. The red solid and blue dashed lines correspond to $\sigma_{\text{SI}}^{\text{LO}}$ and $\sigma_{\text{SI}}^{\text{NLO}}$, respectively. The black dashed and green dashed lines are separately constraints given by the PandaX-II [9] and XENON1T [8] experiments. One can conclude from the plot that even though the $\sigma_{\text{SI}}^{\text{LO}}$ is suppressed by the dark matter velocity it is still sizable and the current constraints have excluded the low dark matter mass region ($6 \text{ GeV} m_\chi < 120 \text{ GeV}$). The next-to-leading contribution is reachable by the current DD technique for light MDM, and it is about 5 orders smaller than the LO term for heavy MDM. The reason that σ^{NLO} being sensitive to light MDM is that σ^{NLO} is proportional to g_V^8 while σ^{LO} is proportional g_V^4 . As a result, a slight increase of g_V may enhance the σ^{NLO} obviously.

We show in the left-panel of the Fig. 6 the spin-dependent χ -neutron scattering cross section as the function of m_χ for scenario B, by setting $\zeta = 1$ and $m_V = 3$ TeV. The blue and green dotted lines are constraints of PandaX-II [56] and XENON1T [57] experiments, respectively. One can see that the mass region (8, 90) GeV is already excluded. We show in the right-panel of the Fig. 6 the spin-independent cross section as the function of m_χ for scenario B. The solid and dashed lines correspond to $m_V = 3$ TeV and 0.5 TeV, respectively. The black solid line is the neutrino floor. It is clear that the spin-independent cross section is too small to be detected in the near future for heavy MDM, but it is detectable for light MDM. σ^{NLO} is a good supplement to the σ^{SD} in detecting light MDM.

V. CONCLUSION

In this paper we have discussed the direct detection cross section of Majorana dark matter χ in the vector portal. At the leading order, the cross section is either velocity suppressed or spin-dependent, and current constraints given by XENON1T and PandaX-II experiments can only rule out a narrow mass range depending on the inputs. Future

direct detection experiments may improve the detection sensitivity to higher level. Next-to-leading order corrections may turn out to be important. We have derived the effective χ -quark interactions at the one-loop level and the effective χ -gluon interaction at the two-loop level. Our numerical results show that the next-to-leading order corrections to the SI cross section is reachable by the current detecting technique for light MDM. Notice that we did not consider constraints of LHC [60] since we are focused on DDs in underground laboratories in this paper, however constraints from collider are definitely important when considering a specific vector portal MDM model.

ACKNOWLEDGMENTS

This work was supported by the National Natural Science Foundation of China under grant No. 11775025 and the Fundamental Research Funds for the Central Universities under grant No. 2017NT17.

Appendix A: Integrations

We list in this appendix definitions of integration used in this paper, given by [46]:

$$\int \frac{d^4k}{(2\pi)^4} \frac{1}{[(p+k)^2 - M_\chi^2]k^2[k^2 - m_V^2]} = \frac{i}{16\pi^2} X_2(p^2, M_\chi^2, 0, m_V^2) \quad (\text{A1})$$

$$\int \frac{d^4k}{(2\pi)^4} \frac{k_\mu}{[(p+k)^2 - M_\chi^2]k^2[k^2 - m_V^2]} = \frac{i}{16\pi^2} p_\mu Y_2(p^2, M_\chi^2, 0, m_V^2) \quad (\text{A2})$$

$$\int \frac{d^4k}{(2\pi)^4} \frac{k_\mu k_\nu}{[(p+k)^2 - M_\chi^2]k^4[k^2 - m_V^2]} = \frac{i}{16\pi^2} [p_\mu p_\nu Z_{11}(p^2, M_\chi^2, m_V^2) + g_{\mu\nu} Z_{00}(p^2, M_\chi^2, m_V^2)] \quad (\text{A3})$$

$$\int \frac{d^4k}{(2\pi)^4} \frac{k_\mu k_\nu k_\sigma}{[(p+k)^2 - M_\chi^2]k^4[k^2 - m_V^2]} = \frac{i}{16\pi^2} [p_\mu p_\nu p_\sigma Z_{111}(p^2, M_\chi^2, m_V^2) + (g_{\mu\nu} p_\sigma + g_{\mu\sigma} p_\nu + g_{\nu\sigma} p_\mu) Z_{000}(p^2, M_\chi^2, m_V^2)] \quad (\text{A4})$$

These integrations are evaluated using package-X [48, 49].

Appendix B: Nuclear form factor

To calculate the WIMP-nucleon scattering cross section, one needs following nuclear form factors: $\langle N | m_q \bar{q}q | N \rangle = m_N f_{T_q}^N$, ($q = u, d, s$), $\langle N | -\frac{9\alpha_s}{8\pi} G_{\mu\nu}^a G^{a\mu\nu} | N \rangle = m_N f_{T_g}^N$, $\langle N | \mathcal{O}_{\mu\nu}^q | N \rangle =$

$\frac{1}{m_N}(p_\mu^N p_\nu^N - \frac{1}{4}m_N^2 g_{\mu\nu})(q^N(2) + \bar{q}^N(2))$, where m_N is nucleon mass, $f_{T_q}^N$ and $f_{T_g}^N$ are form factors taken from micrOmegas [58], $q^N(2)$ and $\bar{q}^N(2)$ are the second momentum for quark distribution functions evaluated at $\mu = m_Z$ by using CTEQ PDF [59]. Specific inputs are [58]

$$f_{T_u}^p = 0.0153, \quad f_{T_d}^p = 0.0191, \quad f_{T_s}^p = 0.0447, \quad (\text{B1})$$

$$f_{T_u}^n = 0.0110, \quad f_{T_d}^n = 0.0273, \quad f_{T_s}^n = 0.0447, \quad (\text{B2})$$

$$f_{T_g}^N = 1 - \sum_{q=u,d,s} f_{T_q}^N, \text{ and [37, 59]}$$

$$u^p(2) = 0.220, \quad d^p(2) = 0.110, \quad s^p(2) = 0.026, \quad c^p(2) = 0.019, \quad b^p(2) = 0.012, \quad (\text{B3})$$

$$\bar{u}^p(2) = 0.034, \quad \bar{d}^p(2) = 0.036, \quad \bar{s}^p(2) = 0.026, \quad \bar{c}^p(2) = 0.019, \quad \bar{b}^p(2) = 0.012. \quad (\text{B4})$$

-
- [1] N. Aghanim *et al.* [Planck Collaboration], arXiv:1807.06209 [astro-ph.CO].
- [2] H. Goldberg, Phys. Rev. Lett. **50**, 1419 (1983) Erratum: [Phys. Rev. Lett. **103**, 099905 (2009)]. doi:10.1103/PhysRevLett.103.099905, 10.1103/PhysRevLett.50.1419
- [3] J. R. Ellis, J. S. Hagelin, D. V. Nanopoulos, K. A. Olive and M. Srednicki, Nucl. Phys. B **238**, 453 (1984). doi:10.1016/0550-3213(84)90461-9
- [4] G. Jungman, M. Kamionkowski and K. Griest, Phys. Rept. **267**, 195 (1996) doi:10.1016/0370-1573(95)00058-5 [hep-ph/9506380].
- [5] G. Servant and T. M. P. Tait, Nucl. Phys. B **650**, 391 (2003) doi:10.1016/S0550-3213(02)01012-X [hep-ph/0206071].
- [6] H. C. Cheng, J. L. Feng and K. T. Matchev, Phys. Rev. Lett. **89**, 211301 (2002) doi:10.1103/PhysRevLett.89.211301 [hep-ph/0207125].
- [7] G. Bertone, D. Hooper and J. Silk, Phys. Rept. **405**, 279 (2005) doi:10.1016/j.physrep.2004.08.031 [hep-ph/0404175].
- [8] D. S. Akerib *et al.* [LUX Collaboration], Phys. Rev. Lett. **112**, 091303 (2014) doi:10.1103/PhysRevLett.112.091303 [arXiv:1310.8214 [astro-ph.CO]].
- [9] A. Tan *et al.* [PandaX-II Collaboration], Phys. Rev. Lett. **117**, no. 12, 121303 (2016) doi:10.1103/PhysRevLett.117.121303 [arXiv:1607.07400 [hep-ex]].
- [10] E. Aprile *et al.* [XENON Collaboration], Phys. Rev. Lett. **119**, no. 18, 181301 (2017) doi:10.1103/PhysRevLett.119.181301 [arXiv:1705.06655 [astro-ph.CO]].

- [11] J. Billard, L. Strigari and E. Figueroa-Feliciano, *Phys. Rev. D* **89**, no. 2, 023524 (2014) doi:10.1103/PhysRevD.89.023524 [arXiv:1307.5458 [hep-ph]].
- [12] E. Dudas, Y. Mambrini, S. Pokorski and A. Romagnoni, *JHEP* **0908**, 014 (2009) doi:10.1088/1126-6708/2009/08/014 [arXiv:0904.1745 [hep-ph]].
- [13] H. An, X. Ji and L. T. Wang, *JHEP* **1207**, 182 (2012) doi:10.1007/JHEP07(2012)182 [arXiv:1202.2894 [hep-ph]].
- [14] M. T. Frandsen, F. Kahlhoefer, A. Preston, S. Sarkar and K. Schmidt-Hoberg, *JHEP* **1207**, 123 (2012) doi:10.1007/JHEP07(2012)123 [arXiv:1204.3839 [hep-ph]].
- [15] H. Dreiner, D. Schmeier and J. Tattersall, *EPL* **102**, no. 5, 51001 (2013) doi:10.1209/0295-5075/102/51001 [arXiv:1303.3348 [hep-ph]].
- [16] A. Alves, S. Profumo and F. S. Queiroz, *JHEP* **1404**, 063 (2014) doi:10.1007/JHEP04(2014)063 [arXiv:1312.5281 [hep-ph]].
- [17] G. Arcadi, Y. Mambrini, M. H. G. Tytgat and B. Zaldivar, *JHEP* **1403**, 134 (2014) doi:10.1007/JHEP03(2014)134 [arXiv:1401.0221 [hep-ph]].
- [18] O. Lebedev and Y. Mambrini, *Phys. Lett. B* **734**, 350 (2014) doi:10.1016/j.physletb.2014.05.025 [arXiv:1403.4837 [hep-ph]].
- [19] N. F. Bell, Y. Cai, R. K. Leane and A. D. Medina, *Phys. Rev. D* **90**, no. 3, 035027 (2014) doi:10.1103/PhysRevD.90.035027 [arXiv:1407.3001 [hep-ph]].
- [20] A. Alves, A. Berlin, S. Profumo and F. S. Queiroz, *Phys. Rev. D* **92**, no. 8, 083004 (2015) doi:10.1103/PhysRevD.92.083004 [arXiv:1501.03490 [hep-ph]].
- [21] A. De Simone and T. Jacques, *Eur. Phys. J. C* **76**, no. 7, 367 (2016) doi:10.1140/epjc/s10052-016-4208-4 [arXiv:1603.08002 [hep-ph]].
- [22] M. Fairbairn, J. Heal, F. Kahlhoefer and P. Tunney, *JHEP* **1609**, 018 (2016) doi:10.1007/JHEP09(2016)018 [arXiv:1605.07940 [hep-ph]].
- [23] Y. Cui and F. D'Eramo, *Phys. Rev. D* **96**, no. 9, 095006 (2017) doi:10.1103/PhysRevD.96.095006 [arXiv:1705.03897 [hep-ph]].
- [24] A. L. Fitzpatrick, W. Haxton, E. Katz, N. Lubbers and Y. Xu, *JCAP* **1302**, 004 (2013) doi:10.1088/1475-7516/2013/02/004 [arXiv:1203.3542 [hep-ph]].
- [25] N. Anand, A. L. Fitzpatrick and W. C. Haxton, *Phys. Rev. C* **89**, no. 6, 065501 (2014) doi:10.1103/PhysRevC.89.065501 [arXiv:1308.6288 [hep-ph]].

- [26] U. Haisch and F. Kahlhoefer, JCAP **1304**, 050 (2013) doi:10.1088/1475-7516/2013/04/050 [arXiv:1302.4454 [hep-ph]].
- [27] A. Crivellin and U. Haisch, Phys. Rev. D **90**, 115011 (2014) doi:10.1103/PhysRevD.90.115011 [arXiv:1408.5046 [hep-ph]].
- [28] F. D’Eramo, B. J. Kavanagh and P. Panci, JHEP **1608**, 111 (2016) doi:10.1007/JHEP08(2016)111 [arXiv:1605.04917 [hep-ph]].
- [29] A. Crivellin, F. D’Eramo and M. Procura, Phys. Rev. Lett. **112**, 191304 (2014) doi:10.1103/PhysRevLett.112.191304 [arXiv:1402.1173 [hep-ph]].
- [30] F. Bishara, J. Brod, B. Grinstein and J. Zupan, arXiv:1809.03506 [hep-ph].
- [31] T. Li, Phys. Lett. B **782**, 497 (2018) doi:10.1016/j.physletb.2018.05.073 [arXiv:1804.02120 [hep-ph]].
- [32] N. F. Bell, G. Busoni and I. W. Sanderson, JCAP **1808**, no. 08, 017 (2018) Erratum: [JCAP **1901**, no. 01, E01 (2019)] doi:10.1088/1475-7516/2018/08/017, 10.1088/1475-7516/2019/01/E01 [arXiv:1803.01574 [hep-ph]].
- [33] J. Hisano, K. Ishiwata and N. Nagata, Phys. Lett. B **690**, 311 (2010) doi:10.1016/j.physletb.2010.05.047 [arXiv:1004.4090 [hep-ph]].
- [34] J. Hisano, K. Ishiwata, N. Nagata and T. Takesako, JHEP **1107**, 005 (2011) doi:10.1007/JHEP07(2011)005 [arXiv:1104.0228 [hep-ph]].
- [35] F. Ertas and F. Kahlhoefer, arXiv:1902.11070 [hep-ph].
- [36] K. Ishiwata and T. Toma, JHEP **1812**, 089 (2018) doi:10.1007/JHEP12(2018)089 [arXiv:1810.08139 [hep-ph]].
- [37] T. Abe, M. Fujiwara and J. Hisano, JHEP **1902**, 028 (2019) doi:10.1007/JHEP02(2019)028 [arXiv:1810.01039 [hep-ph]].
- [38] W. Chao, G. J. Ding, X. G. He and M. Ramsey-Musolf, arXiv:1812.07829 [hep-ph].
- [39] J. Hisano, R. Nagai and N. Nagata, JHEP **1505**, 037 (2015) doi:10.1007/JHEP05(2015)037 [arXiv:1502.02244 [hep-ph]].
- [40] J. Hisano, arXiv:1712.02947 [hep-ph].
- [41] J. Hisano, K. Ishiwata and N. Nagata, Phys. Rev. D **82**, 115007 (2010) doi:10.1103/PhysRevD.82.115007 [arXiv:1007.2601 [hep-ph]].
- [42] J. Hisano, K. Ishiwata and N. Nagata, JHEP **1506**, 097 (2015) doi:10.1007/JHEP06(2015)097 [arXiv:1504.00915 [hep-ph]].

- [43] R. N. Mohapatra and R. E. Marshak, Phys. Rev. Lett. **44**, 1316 (1980) Erratum: [Phys. Rev. Lett. **44**, 1643 (1980)]. doi:10.1103/PhysRevLett.44.1644.2, 10.1103/PhysRevLett.44.1316
- [44] W. Chao, H. k. Guo and Y. Zhang, JHEP **1704**, 034 (2017) doi:10.1007/JHEP04(2017)034 [arXiv:1604.01771 [hep-ph]].
- [45] W. Chao, Eur. Phys. J. C **78**, no. 2, 103 (2018) doi:10.1140/epjc/s10052-018-5547-0 [arXiv:1707.07858 [hep-ph]].
- [46] T. Abe and R. Sato, JHEP **1503**, 109 (2015) doi:10.1007/JHEP03(2015)109 [arXiv:1501.04161 [hep-ph]].
- [47] D. Adams *et al.* [Spin Muon Collaboration], Phys. Lett. B **357**, 248 (1995). doi:10.1016/0370-2693(95)00898-U
- [48] H. H. Patel, Comput. Phys. Commun. **197**, 276 (2015) doi:10.1016/j.cpc.2015.08.017 [arXiv:1503.01469 [hep-ph]].
- [49] H. H. Patel, Comput. Phys. Commun. **218**, 66 (2017) doi:10.1016/j.cpc.2017.04.015 [arXiv:1612.00009 [hep-ph]].
- [50] V. A. Novikov, M. A. Shifman, A. I. Vainshtein and V. I. Zakharov, Fortsch. Phys. **32**, 585 (1984).
- [51] V. Shtabovenko, R. Mertig and F. Orellana, Comput. Phys. Commun. **207**, 432 (2016) doi:10.1016/j.cpc.2016.06.008 [arXiv:1601.01167 [hep-ph]].
- [52] F. D'Eramo and M. Procura, JHEP **1504**, 054 (2015) doi:10.1007/JHEP04(2015)054 [arXiv:1411.3342 [hep-ph]].
- [53] R. J. Hill and M. P. Solon, Phys. Rev. D **91**, 043504 (2015) doi:10.1103/PhysRevD.91.043504 [arXiv:1401.3339 [hep-ph]].
- [54] R. J. Hill and M. P. Solon, Phys. Rev. D **91**, 043505 (2015) doi:10.1103/PhysRevD.91.043505 [arXiv:1409.8290 [hep-ph]].
- [55] K. A. Mohan, D. Sengupta, T. M. P. Tait, B. Yan and P. Yuan, arXiv:1903.05650 [hep-ph].
- [56] C. Fu *et al.* [PandaX-II Collaboration], Phys. Rev. Lett. **118**, no. 7, 071301 (2017) Erratum: [Phys. Rev. Lett. **120**, no. 4, 049902 (2018)] doi:10.1103/PhysRevLett.120.049902, 10.1103/PhysRevLett.118.071301 [arXiv:1611.06553 [hep-ex]].
- [57] E. Aprile *et al.* [XENON Collaboration], Phys. Rev. Lett. **122**, no. 14, 141301 (2019) doi:10.1103/PhysRevLett.122.141301 [arXiv:1902.03234 [astro-ph.CO]].

- [58] G. Blanger, F. Boudjema, A. Goudelis, A. Pukhov and B. Zaldivar, *Comput. Phys. Commun.* **231**, 173 (2018) doi:10.1016/j.cpc.2018.04.027 [arXiv:1801.03509 [hep-ph]].
- [59] J. Pumplin, D. R. Stump, J. Huston, H. L. Lai, P. M. Nadolsky and W. K. Tung, *JHEP* **0207**, 012 (2002) doi:10.1088/1126-6708/2002/07/012 [hep-ph/0201195].
- [60] M. Aaboud *et al.* [ATLAS Collaboration], arXiv:1903.01400 [hep-ex].